Refractive index of Ag nanocrystals composite films in the neighborhood of the surface plasmon resonance

J. C. G. de Sande, R. Serna, J. Gonzalo, C. N. Afonso, D. E. Hole et al.

Citation: J. Appl. Phys. **91**, 1536 (2002); doi: 10.1063/1.1427404

View online: http://dx.doi.org/10.1063/1.1427404

View Table of Contents: http://jap.aip.org/resource/1/JAPIAU/v91/i3

Published by the American Institute of Physics.

Refractive index of Ag nanocrystals composite films in the neighborhood of the surface plasmon resonance

J. C. G. de Sande[a)]
Ingeniería de Circuitos y Sistemas, E.U.I.T.T., U.P.M., Ctra. de Valencia km 7.5, 28031 Madrid, Spain

R. Serna, J. Gonzalo, and C. N. Afonso
Instituto de Optica, CSIC, Serrano 121, 28006 Madrid, Spain

D. E. Hole
School of Engineering, Pevensey Building, University of Sussex, Brighton, BN1 9QH, United Kingdom

A. Naudon
Laboratoire de Métallurgie Physique, URA 6630 du CNRS, UFR Sciences, Bat. SP2MI; Boulevard 3, Téléport 2, BP 179, 86960 Futuroscope Cedex, France

(Received 28 March 2001; accepted for publication 22 October 2001)

Nanocomposite thin films formed by Ag nanocrystals embedded in an amorphous aluminum oxide (Al_2O_3) host were prepared by alternating-target pulsed laser deposition. Spectroscopic ellipsometry was used to determine the effective refractive index ($\mathbf{n}=n+ik$). When the Ag volume fraction is over 2%, the linear optical properties of the nanocomposite films differ from those of the pure dielectric host. The extinction coefficient shows a maximum around 435 nm that is related to the surface plasmon resonance. Near this wavelength, the real part of the refractive index undergoes anomalous dispersion, leading to a significant increase of the *n* value of the composite compared to that of the matrix. © *2002 American Institute of Physics.* [DOI: 10.1063/1.1427404]

INTRODUCTION

For centuries, metal nanocrystals (NCs) have been embedded in dielectric transparent matrices to produce colored glassware. Their optical response arises from the excitation of surface plasmons in the metal NCs that induces a selective enhancement of absorption. The frequency of the surface plasmon resonance (SPR) depends on the dielectric properties of the metal and the embedding medium, as well as on the size, size distribution, and shape of the NCs. The special optical properties of these nanocomposite systems are attractive for a wide range of technological applications, such as functional optical coatings (e.g., selective solar absorbers),[1,2] broadband waveguide polarizers,[3] and ultrafast optical switches, the latter due to an enhanced third order nonlinear optical susceptibility [$\chi^{(3)}$] with time response of a few picoseconds.[4–6]

For all applications, knowledge of the linear optical properties ($\mathbf{n}=n+ik$) is necessary to design suitable devices. Nevertheless, the real part of the refractive index (n) has rarely been studied, as attention is usually directed to the characteristic SPR feature in the extinction coefficient (k) spectrum.[7–9] The knowledge of n, however, is essential to obtain the required index-matching in waveguide devices. Moreover, all nonlinear optical characterization techniques, such as *Z*-scan or four-wave mixing, depend on knowing the n value of the composite to determine the nonlinear refractive index.[10–12] In the literature, it is most common to use the refractive index of the matrix with no NCs.[12] This approach is not accurate since the real part of the effective linear refractive index of the nanocomposite around the SPR suffers a great modification compared to that of the matrix. In addition, special care has to be taken if studies as a function of the wavelength are performed, since the spectral response is also affected by the presence of the NCs.

The aim of this work is to determine by spectroscopic ellipsometry (SE) the effective linear refractive index, both the real and imaginary parts ($\mathbf{n}=n+ik$), of the nanocomposite system formed by Ag NCs embedded in an amorphous aluminum oxide (Al_2O_3) matrix as a function of Ag metal content. SE has unquestionable advantages when compared to standard transmission measurements, because both real and imaginary parts of the refractive index of a homogeneous material can be directly obtained in a single measurement operation on a wavelength-by-wavelength basis. In addition it will be shown that SE measurements together with the standard Bruggeman effective medium model yield the volume fraction of metal in the films.

EXPERIMENT

Ag:Al_2O_3 thin films were prepared by alternating-target pulsed laser deposition (PLD) using an ArF excimer laser ($\tau=20$ ns full width at half maximum (FWHM), $\lambda=193$ nm, 10 Hz repetition rate) focused at 45° angle of incidence on high-purity Al_2O_3 and Ag targets. The targets were placed into a computer-controlled holder for sequential ablation. The laser fluence on the targets was 2 J/cm^2. The films were grown at room temperature on chemically cleaned Si substrates 32 mm away on the normal to the target. The vacuum chamber base pressure during deposition was 7×10^{-7} Torr.

The synthesis consists of sequential growth of an Al_2O_3 layer followed by deposition of the Ag NCs, repeated five

a)Electronic mail: jcgsande@ics.upm.es

TABLE I. Number of pulses on Ag target per layer (N), total Ag areal density ([Ag]) measured by RBS, thickness and Ag volume content obtained from RBS, average diameter of the NCs (ϕ) obtained from GISAXS and standard deviation, thickness, and Ag volume content from SE. The thickness of the film and the Ag concentration in volume percent in the column "RBS" have been calculated from the areal atomic density measured by RBS and assuming the Ag bulk density and the amorphous alumina density determined in Ref. 17. The standard deviation σ is a measure of the quality of the fit.

FILMS	RBS			GISAXS	SE		
N	[Ag] ($\times 10^{15}$ at/cm^2)	Thickness (nm)	Ag vol %	ϕ (nm)	σ	Thickness (nm)	Ag vol %
25	2.5	150 ± 6	0.28	⋯	0.06	133	0.03
75	3.6	150 ± 6	0.41	1.0	0.06	131	0.06
100	5.0	150 ± 6	0.56	2.0	0.09	131	0.22
150	20	150 ± 6	2.20	3.9	0.09	132	2.15
200	31	140 ± 6	3.81	5.9	0.18	124	4.27

times. Finally, a layer of Al_2O_3 was deposited to protect the Ag against atmospheric contact. The number of pulses on each target determines the thickness of the Al_2O_3 layer and the Ag content. The selected thickness for the Al_2O_3 spacing layers was 25 ± 5 nm, and the number of pulses on the Ag target was varied from 25 to 200 pulses. The Ag content of the film was determined by Rutherford backscattering spectrometry (RBS) using a 2.0 MeV $^4He^+$ beam and the experimental spectra were simulated using the RUMP program.[13] The average dimensions of the Ag aggregates were determined by small angle x-ray scattering (GISAXS). The energy was set to 8049 eV, corresponding to a wavelength of 0.154 nm. The distance between the sample and the detector was 650 nm and the angle of incidence was slightly higher that the critical angle of the films ($\theta\approx0.22°$) in order to penetrate into the layer.[14] The crystalline structure of the Ag aggregates was observed by transmission electron microscopy, thus confirming that they are NCs, as was found in earlier work on the synthesis of Cu and Bi NCs by PLD.[5,15,16]

The ellipsometric parameters $\tan\psi$ and $\cos\delta$ were measured by a SOPRA spectroscopic rotating polarizer ellipsometer in the 300–700 nm wavelength range using steps of 5 nm, at an angle of incidence of $(70.07\pm0.05)°$. The standard deviations of ten measured $\tan\psi$ and $\cos\delta$ values at the same wavelength for each sample were typically lower than 5×10^{-4} and 10^{-3}, respectively.

The optical properties of heterogeneous or composite systems have been successfully modeled in the past by effective medium theories (EMT), typically those of Maxwell–Garnet and Bruggeman.[17–19] In nanocomposite systems, distortions in the microscopic electric field and polarization due to the mixture of different materials give rise to local-field effects and dielectric functions that differ from the simple average over those of the constituents. In earlier studies, we have found that both EMT Maxwell–Garnet and Bruggeman models give similar results for composite films with a low volume fraction of metal NCs, but the Maxwell–Garnett approximation deviates from the experimental data for high volume fraction of metal.[5,17] In the latter case, the Bruggeman approximation is more representative.[8,18,19] This model follows a self- consistent approach in which the effective medium acts itself as the host, following the expression:

$$0=f_m\frac{\epsilon_m-\epsilon_{\text{eff}}}{\epsilon_m+2\epsilon_{\text{eff}}}+f_d\frac{\epsilon_d-\epsilon_{\text{eff}}}{\epsilon_d+2\epsilon_{\text{eff}}}, \tag{1}$$

where ϵ_{eff}, ϵ_m, and ϵ_d are the dielectric functions of the effective medium, the metal, and the dielectric, and f_m and $f_d=(1-f_m)$ are the volume fractions of the metal and dielectric, respectively. From this equation, the component volume fractions can be determined once the dielectric constants of the two components of the composite are known and the effective dielectric constant of the medium is measured.

The Bruggeman EMT for three-dimensional isotropic systems combined with a standard regression method was used to simulate the measured ellipsometric parameters of the nanocomposite films. An air/(Al_2O_3+Ag)/ substrate system is considered, the film thickness and metal volume fraction in the film being the fitting parameters. We have assumed the optical properties of crystalline bulk Si for the substrate and that of bulk Ag for the NCs.[20] For the amorphous aluminum oxide matrix, we have used our earlier results on amorphous Al_2O_3 films grown by PLD.[17]

RESULTS

Table I includes the total Ag content in the films (areal density, [Ag]) as measured by RBS. [Ag] increases with the number of laser pulses on the Ag target, consistent with our earlier results for Cu and Bi NCs.[5,15,16] The thickness of the films was extracted from the areal density of Al_2O_3 determined by RBS, assuming the density of the amorphous aluminum oxide to be 8.7×10^{22} at/cm^3.[17] The thickness of the films seems to be fairly constant within the experimental error. Assuming that the density of the Ag NCs is the same as that of bulk Ag,[20] the volume fraction of Ag was calculated from the areal density determined by RBS for both the Al_2O_3 and the Ag; it varies from 0.28% to 3.81%. GISAXS measurements show that for films synthesized with [Ag]$>3.6\times10^{15}$ at/cm^2, metal NCs are formed. The average diameter of the NCs (see Table I) increases monotonically from 1.0 to 5.9 nm with increasing [Ag].

Figure 1 shows the measured $\tan\psi$ and $\cos\delta$ values for all the studied films. Samples with [Ag]$<5.0\times10^{15}$ at/cm^2 show a similar behavior throughout the studied spectral

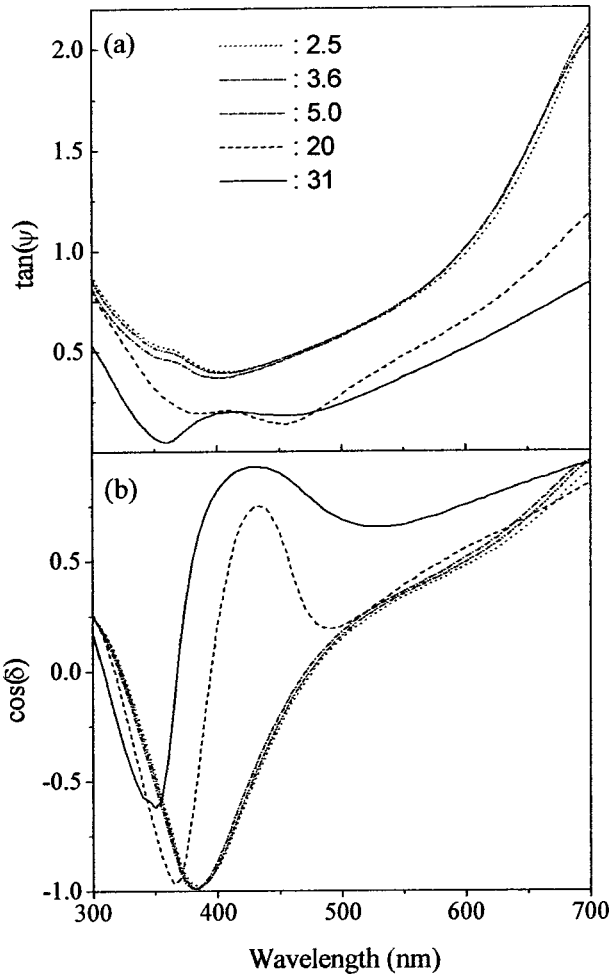

FIG. 1. Measured values of (a) tan ψ and (b) cos δ for all the studied films. Numbers in the inset indicate the measured areal density of Ag ($\times 10^{15}$ at/cm^2).

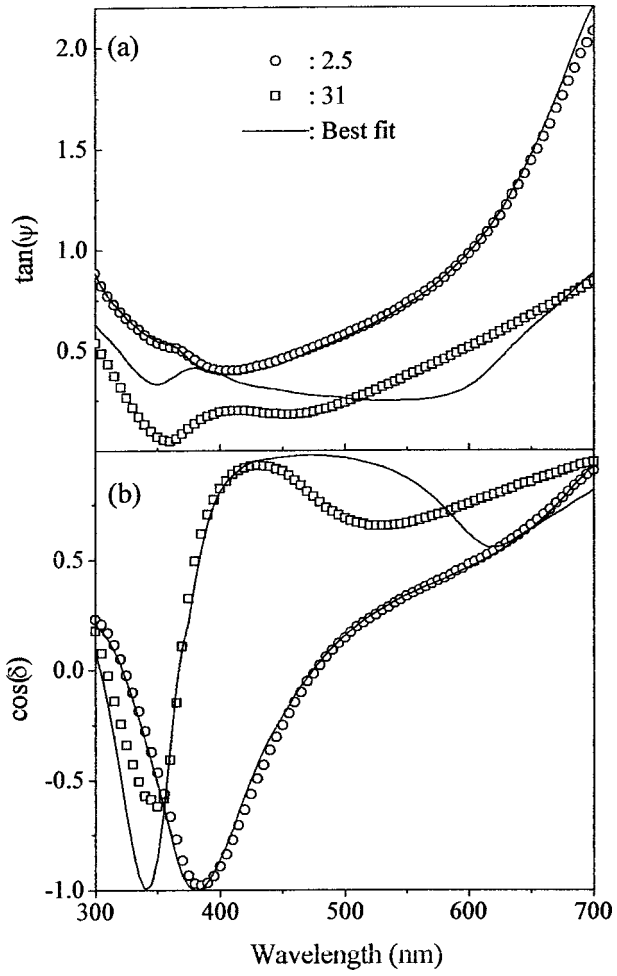

FIG. 2. Fits of the ellipsometric parameters for the samples of lowest and highest Ag content. Symbols represent experimental values and the lines are the best fits. Numbers in the inset indicate the measured areal density of Ag ($\times 10^{15}$ at/cm^2).

range whereas that of samples with [Ag]$>20\times10^{15}$ at/cm^2 is drastically different. This can be clearly appreciated in the behavior of cos δ in the 350–500 nm wavelength range [see Fig. 1(b)], where the measured cos δ for the latter films show a maximum which is not observed in the former ones.

The film thickness and metal volume fraction has also been calculated from the results shown in Fig. 1 using: (i) an air/(Al_2O_3+Ag)/ substrate system, (ii) the Bruggeman EMT (in order to obtain the optical properties of the films from those of its constituents), and (iii) a standard regression method (to fit the measured tan ψ and cos δ values).[17] Figure 2 represents the best fits for the films having the lowest and the highest [Ag]. Whereas the fit for the former is excellent, significant discrepancies appear for that of the latter. The fit specially fails in the 400–600 nm wavelength range, where the maximum and minimum are not in the same positions although the theoretical model gives the general trend of the behavior of the SE parameters. The values of the film thickness and Ag content determined from the best fit for each sample are also listed in Table I. The quality of the fits is given by the standard deviation (σ). As expected from the fits shown in Fig. 2, the confidence in the fit is better the lower the Ag content in the films. The thickness of the films determined from the SE data are systematically lower than those determined from the RBS data. Regarding the Ag volume percent obtained from the analysis of the optical data (last column of Table I), it is noticeable that the ellipsometric measurements do not seem to be very sensitive to the presence of Ag for the lowest [Ag] film. The best agreement for the Ag volume percent content is achieved for the films having the highest [Ag], although the fit is poorer.

Figure 3 shows the real (n) and imaginary (k) parts of the refractive index obtained by numerical inversion from the data shown in Fig. 1 and assuming the film thickness estimated from the SE measurements (Table I).[21] The refractive index of a reference Al_2O_3 film with no NCs is also shown in the figure for comparison.[17] The imaginary part of the refractive index of samples with [Ag]$\leqslant 5.0\times10^{15}$ at/cm^2 or Ag NCs with average diameter <2.0 nm is not drawn because they are beyond the resolution of the measurements (typically lower than 0.01). It is clearly seen that the optical response of the films with low [Ag] is similar to that of the matrix, the only difference being a slightly higher real part of the refractive index. The small structure discontinuities observed in the spectra for values around 360 nm are due to

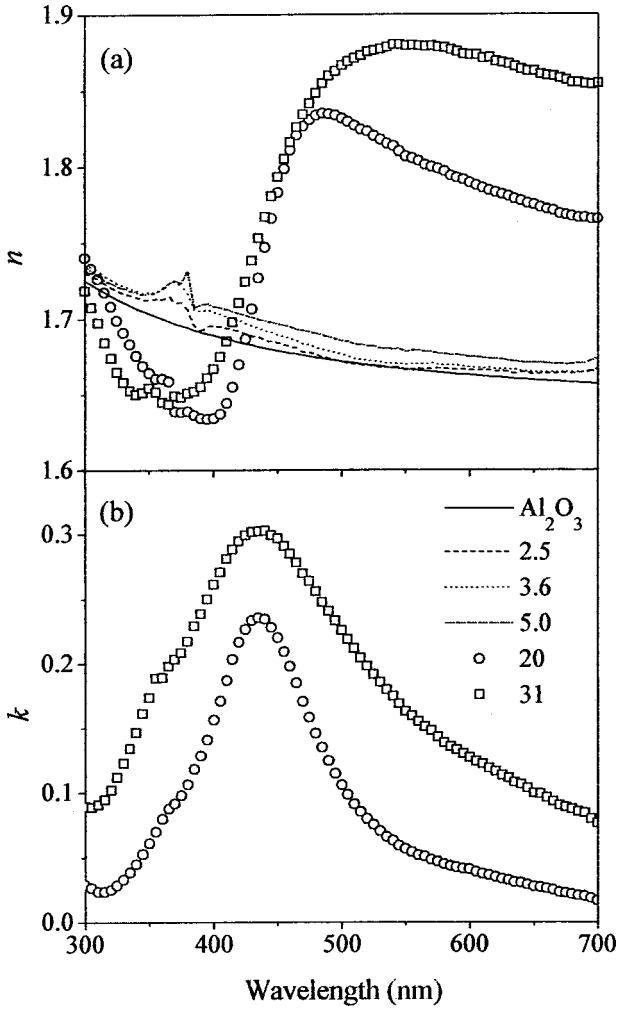

FIG. 3. (a) Real (n) and (b) imaginary (k) parts of the refractive index of all studied films. The imaginary part is only drawn for the two films with the highest Ag content since the other films exhibit negligible extinction coefficient within the experimental resolution. The refractive index of the Al_2O_3 reference film is included for comparison. Numbers in the inset indicate the measured areal density of Ag ($\times 10^{15}$ at/cm^2).

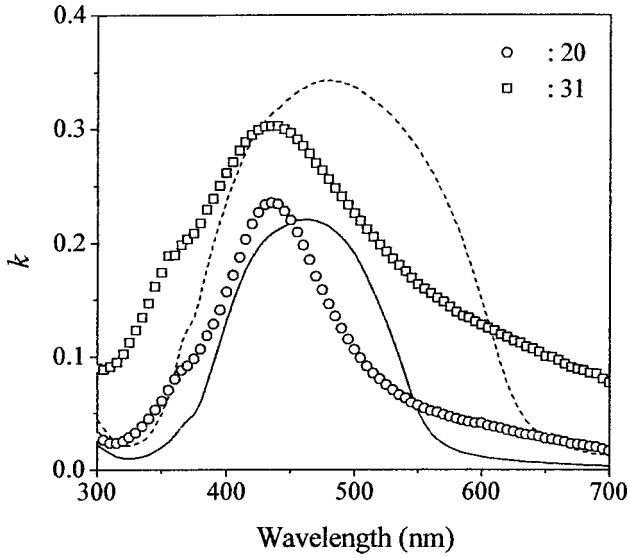

FIG. 4. Extinction coefficient for films with [Ag]$\geqslant 20\times 10^{15}$ at/cm^2 (symbols) and simulation of the extinction coefficient for a mixture with 2.15% (solid line) and 4.27% (dashed line) of Ag in Al_2O_3 matrix calculated by means of the Bruggeman EMT. Numbers in the inset indicates the measured areal density of Ag ($\times 10^{15}$ at/cm^2).

inconsistencies/limitations in the measurement when δ approaches to 0° or 180° ($\cos\delta = \pm 1$).

Samples with [Ag]$\geqslant 20\times 10^{15}$ at/cm^2 and Ag NCs with an average diameter >3.9 nm, show new interesting features. The imaginary part (k) is not negligible and presents a broadband centered around 435 nm related to the SPR absorption.[8] The extinction coefficient peak for the two high composition films studied is at the same spectral position within experimental resolution (± 5 nm). In addition, there is an increase in the SPR FWHM from 110 to 220 nm (or from 0.71 to 1.42 eV, respectively) as the [Ag] increases from 20×10^{15} at/cm^2 to 31×10^{15} at/cm^2. The real part of the refractive index (n) also shows a quite different behavior than that of pure Al_2O_3 films, since n undergoes a sharp increase at the wavelengths at which the SPR band occurs. Besides, the n value for longer wavelengths is significantly higher than that of the reference Al_2O_3 film.

Figure 4 compares between the extinction coefficients obtained from the SE measurements of films with [Ag]$\geqslant 20\times 10^{15}$ at/cm^2 and those simulated by means of the Bruggeman EMT for films having 2.15% and 4.27% Ag volume content. The simulation only gives the general trend of the measured extinction coefficient, since the peak position and shape of the SPR are somewhat different from those determined by SE measurements. The extinction coefficients simulated by means of the Bruggeman EMT show a redshift of the SPR maximum from 460 to 480 nm as opposed to the constant value obtained from the SE measurements. The FWHM of the SPR band obtained by the Bruggeman EMT increases from 135 to 210 nm (or from 0.81 to 1.15 eV, respectively) as [Ag] increases, this increase having the same sign and similar amplitude as that obtained by the SE measurements.

DISCUSSION

Figures 1 and 3 clearly show that the optical response of Ag:Al_2O_3 nanocomposite films changes when [Ag] increases from 5 to 20×10^{15} at/cm^2. We will thus discuss separately the results obtained for films having [Ag] below and above this interval that will be referred from now on as low and high Ag content films.

The spectral dependence of the real part of the refractive index for low Ag content films is very similar (Fig. 3), the only significant difference being an overall increase of n as the Ag content is increased. Since this behavior is very similar to the one observed when the optical density of the films changes, we have tried to fit the ellipsometric parameters by assuming the films are formed by a mixture of Al_2O_3 and voids, leading to an air/(Al_2O_3 $\pm$ voids)/substrate system. The fits obtained are in very good agreement with the data shown in Fig. 1 for the low Ag content films ([Ag]$\leqslant 5\times 10^{15}$ at/cm^2). The results show that the films having [Ag]$=2.5$, 3.6, and 5.0×10^{15} at/cm^2, respectively, behave as if they were, respectively, 2.0%, 3.2%, and 5.6% denser than the reference Al_2O_3 film and had practically the same SE thickness as

those reported in Table I. This result suggests that the presence of low volume fractions of Ag in the films is optically equivalent to a film with an increased effective density. In other words, a small Ag content ($[Ag] \leqslant 5\times10^{15}$ at/cm^2) or Ag NCs with average diameters $\leqslant 2.0$ nm lead to a slight increase of the real part of the refractive index while the absorption is kept below resolution.

The system model [air/(Al_2O_3 ± void)/substrate] does not predict the special features observed in both the real and imaginary parts of the refractive index of the films with high Ag content ($[Ag] \geqslant 20\times10^{15}$ at/cm^2). The observed maxima of the extinction coefficient shown in Fig. 3(b) for these films can be qualitatively understood within the exact treatment of the Mie theory for the scattering produced by a conducting sphere in the electric dipole approximation.[9] In the present case (Ag NCs in an Al_2O_3 host), the Mie theory predicts that the peak position of the SPR occurs around 440 nm, which is in very good agreement with the wavelength for which the maximum of k is observed experimentally [Fig. 3(b)].

The observed anomalous dispersion shown in Fig. 3(a) for the real part of the refractive index of the high Ag content films with respect to the refractive index of the pure dielectric host, has scarcely been reported or discussed in the literature. Nevertheless, the experimentally obtained wavelength dependence is consistent with the Kramers–Kronig relations in the sense that the real part of the refractive index is expected to undergo an anomalous dispersion where the extinction coefficient shows a maximum.[8,9,22] Experimentally, a decrease of n for wavelengths shorter than that of the SPR followed by a large increase for longer wavelengths (up to a 13% for the studied films) are observed. As it was pointed out in the introduction, one of the effects of the variation of the linear optical properties of the composite is its influence on the calculation of the third order susceptibility of the material from nonlinear optical measurements. In the case of Z-scan measurements, the estimation of $\chi^{(3)}$ using the refractive index of the pure matrix would lead to a value 27% lower than that obtained with the actual refractive index of the composite having the highest Ag content and thus the largest change in n. Furthermore, when the spectral dependence of $\chi^{(3)}$ is studied, the spectral variations of the n value, that are not normally taken into account, become essential.

The results shown in Fig. 4 show clearly that the Bruggeman EMT does not offer a completely satisfactory explanation of the evolution of the extinction coefficient as a function of [Ag] for the high Ag content films. The SPR maxima obtained from the SE measurements show no significant change in position as [Ag] increases, as opposed to the data obtained from the simulation that exhibited a clear redshift. In addition, the broadening observed in the FWHM of the SPR band, is higher in the case of the SE data than in the simulated curves. These discrepancies suggest that there must be other factors that have a significant influence on the optical behavior of a nanocomposite besides metal fraction, size effects, and interactions between the NCs and the matrix being the most considered ones.[6,8,9,18,23] Experimentally, the peak position and the FWHM of the SPR has been widely studied for metal NCs embedded in dielectric matrices,[7,8,9,24] and different behaviors have been reported depending on the NC size and the nature of the matrix. It has been shown that for very small NCs (diameter $<5-10$ nm, depending on the embedding media) the peak energy of the SPR does not change, but the width decreases with increasing size,[9] whereas a redshift accompanied by broadening of the SPR has been observed for larger sizes.[7,9,24] Our films contain Ag NCs that belong to the category of ''small size'' (diameter <5.9 nm), and thus the constant peak energy observed is consistent with the expected value for these small NCs. Nevertheless, we observed a broadening instead of the predicted sharpening of the SPR. The reasons for this discrepancy are twofold. On one hand, we have reported earlier that an increase of the size of the NCs produced by PLD is associated with a broadening in the size distribution[5,15,16] that can contribute to the broadening of the SPR band. On the other hand, the SPR widths have been reported to be very large, but without any clear correlation to the cluster size in systems having a matrix with high ionicity.[8,9] The high ionicity of our matrix, Al_2O_3, can thus contribute to the observed broadening.

Finally, it is remarkable that the Ag volume content can be reasonably predicted in our case with the Bruggeman EMT using the air/(Al_2O_3+Ag)/substrate system model for the high Ag content films, in spite of the poor fit obtained (Figs. 2 and 4). The reasons why such a satisfactory estimation of the metal content is achieved might be related to the fact that the SE parameters of the high Ag content films in the region away from the SPR wavelength, are not significantly different from those of the low Ag content films (see Fig. 1 for wavelengths shorter than 350 nm or longer than 500 nm). This indicates that the behavior of the NCs can be well described by the dielectric constants of bulk Ag for the low and high wavelength regions in respect to the SPR. In other words, the effective medium theories can be used as a reasonable approximation to the behavior of the optical properties of the nanocomposite away from the resonance.

CONCLUSIONS

Spectroscopic ellipsometry has been used to determine by direct numerical inversion the optical constants, both n and k values, of nanocomposite films formed by Ag metal NCs embedded in a dielectric Al_2O_3 host. The behavior of the refractive index of the material compared to that of the pure dielectric host shows a great change for films with [Ag] $\geqslant 20\times10^{15}$ at/cm^2 that have NCs with an average diameter $\geqslant 3.9$ nm. This change is related to the appearance of both a maximum in the extinction coefficient of the nanocomposite (SPR) and an anomalous dispersion in the real part of the refractive index. The inclusion of NCs leads to a significant variation (up to a 13% for the studied films) of the real part of the refractive index in respect to that of the pure dielectric host. Finally, it is shown that the Bruggeman EMT can be used to estimate the metal fraction in the films with [Ag] $\geqslant 20\times10^{15}$ at/cm^2 (or $\geqslant 2.2\%$ in volume) but it fails to describe the spectral features in the neighborhood of the SPR.

ACKNOWLEDGMENTS

Professor E. Bernabeu (UCM, Spain) is thanked for provision of spectroscopic ellipsometry facilities. The authors are grateful to the technical staff of LURE–DCI for providing the synchrotron beam and for assistance during the GISAXS experiment. This work has been partially supported by TIC99-0866, CICYT (Spain) and by the E.U. under the BRITE Project No. BRPR-CT98-0616.

[1] R. Joerger, R. Gampp, A. Heinzel, W. Graf, M. Köhl, P. Gantenbein, and P. Oelhafen, Sol. Energy Mater. Sol. Cells **54**, 351 (1998).
[2] W. F. Bogaerts and C. M. Lampert, J. Mater. Sci. **18**, 2847 (1983).
[3] M. J. Bloemer and J. W. Haus, J. Lightwave Technol. **14**, 1534 (1996).
[4] Y. Hamanaka, A. Nakamura, S. Omi, N. Del Fatti, F. Vallée, and C. Flytzanis, Appl. Phys. Lett. **75**, 1712 (1999).
[5] C. N. Afonso, J. Solís, R. Serna, J. Gonzalo, J. M. Ballesteros, and J. C. de Sande, Proc. SPIE **3618**, 453 (1999).
[6] Y. Takeda, V. T. Gritsyna, N. Umeda, C. G. Lee, and N. Kishimoto, Nucl. Instrum. Methods Phys. Res. B **148**, 1029 (1999).
[7] S. Banerjee and D. Chakravorty, Appl. Phys. Lett. **72**, 1027 (1998).
[8] H. Hövel, S. Fritz, A. Hilger, U. Kreibig, and M. Vollmer, Phys. Rev. B **48**, 18178 (1993).
[9] U. Kreibig and M. Vollmer, *Optical Properties of Metal Clusters* (Springer, Berlin, 1995).
[10] M. Sheik-Bahae, A. A. Said, T.-H. Wei, D. J. Hagan, and E. W. VanStryland, IEEE J. Quantum Electron. **26**, 760 (1990).
[11] R. F. Haglund, L. Yang, R. H. Magruder III, J. E. Wittig, K. Becker, and R. A. Zuhr, Opt. Lett. **18**, 373 (1993).
[12] L. Yang *et al.*, J. Opt. Soc. Am. B **11**, 457 (1994).
[13] L. R. Doolite, Nucl. Instrum. Methods Phys. Res. B **9**, 344 (1985).
[14] A. Naudon and D. Thiaudiere, J. Appl. Crystallogr. **30**, 822 (1997).
[15] R. Serna, C. N. Afonso, J. M. Ballesteros, A. Naudon, D. Babonneau, and A. K. Petford-Long, Appl. Surf. Sci. **138**, 1 (1999).
[16] R. Serna, T. Missana, C. N. Afonso, J. M. Ballesteros, A. K. Petford-Long, and R. C. Doole, Appl. Phys. A: Mater. Sci. Process. **66**, 43 (1998).
[17] R. Serna, J. C. G. de Sande, J. M. Ballesteros, and C. N. Afonso, J. Appl. Phys. **84**, 4509 (1998).
[18] D. Dalacu and L. Martinu, J. Vac. Sci. Technol. A **17**, 877 (1999).
[19] D. E. Aspnes, in *Handbook of Optical Constants of Solids*, edited by E. D. Palik (Academic, San Diego, CA, 1998), Chap. 5, pp. 89–112.
[20] *Handbook of Optical Constants of Solids*, edited by E. D. Palik (Academic, San Diego, CA, 1998).
[21] R. M. A. Azzam and N. M. Bashara, *Ellipsometry and Polarized Light* (North-Holland, Amsterdam, 1977).
[22] A. Yariv, *Optical Electronics in Modern Communications* (Oxford University Press, New York, 1997).
[23] S. Charvet, R. Madelon, F. Gourbilleaou, and R. Rizk, J. Appl. Phys. **85**, 4032 (1999).
[24] Z. Liu, H. Wang, H. Li, and X. Wang, Appl. Phys. Lett. **72**, 1823 (1998).